Magnetic structure of ordered FeAl and FeV

V. L. Moruzzi and P. M. Marcus
IBM Research Division, Thomas J. Watson Research Center, P.O. Box 218, Yorktown Heights, New York 10598
(Received 14 September 1992)

First-principles augmented-spherical-wave fixed-spin-moment solutions of the Kohn-Sham band equations are used to study the volume dependence of the total energy and the local moments in ordered FeAl and FeV. The solutions yield volume ranges with stable ferromagnetic and metastable type-I antiferromagnetic states for both FeAl and FeV, with energy differences less than $\simeq 0.5$ mRy over a wide range of volumes around equilibrium. For FeV, an unstable mixed antiferromagnetic state with equal and opposite iron and vanadium local moments is also found. Solutions corresponding to type-II antiferromagnetism were not found. Near equilibrium iron local moments are $\simeq 0.5\mu_B$ for the antiferromagnetic state, and $\simeq 0.7\mu_B$ for the ferromagnetic state for FeAl, and $\simeq 0.7\mu_B$ for both the ferromagnetic and antiferromagnetic states in FeV. The calculated lattice constant at equilibrium is within 1.8% of the experimental value for FeAl, and within 1.4% for FeV.

I. INTRODUCTION

Binary metallic compounds with the ordered $B2$-type (CsCl) structure are interesting because the basic unit cell contains only two atoms. As a consequence, electronic-structure calculations of the ground state are generally reliable and can be used as a theoretical tool to provide an understanding of their experimental properties. In order to understand the properties of such compounds containing magnetically active constituents, it is necessary to consider magnetic unit cells large enough to allow for antiferromagnetism (AF). In this paper we give results for magnetic ground-state properties of FeAl and extend our previous work on FeV to include AF states. The present study is motivated by the observation that experiment implies that FeAl is nonmagnetic (NM), while FeV has a ferromagnetic (FM) ground state.

Although ordered $B2$-type systems have no near-neighbor atoms of the same kind, compositions that are off stoichiometry will be chemically disordered and will contain some clusters with the same atoms as near neighbors. Experimentally, even the 50%-50% compounds can be chemically disordered so that a theoretical calculation for a perfectly ordered system may not reproduce experiment. For example, although ordered FeAl has no Fe-Fe or Al-Al near neighbors, iron-rich alloys will have some Fe-Fe neighbors, which can strongly affect the magnetic properties. Neutron-scattering studies[1] show that in $Fe_{0.7}Al_{0.3}$, Fe atoms with only Fe near neighbors have magnetic moments of $\simeq 2.18\mu_B$, while Fe atoms with Al near neighbors have moments of $\simeq 1.50\mu_B$. However, before attempting to understand the complex effects of disorder, it is important to know the behavior of the ordered systems.

The phase diagram for the Fe-Al alloys with between 25% and 50% aluminum shows several unusual magnetic features. These alloys are paramagnetic (implying finite but disordered local moments) at high temperatures, are FM in the iron-rich range at intermediate temperatures, and exist in a so-called cluster-glass state with no net moment at low temperatures. Magnetic measurements show[2,3] that $Fe_{0.7}Al_{0.3}$ is paramagnetic above $\simeq 400$ K, exhibits FM order between $\simeq 400$ and $\simeq 170$ K, becomes paramagnetic again between $\simeq 170$ and $\simeq 92$ K, and exhibits complicated spin-glass-like behavior usually described as the formation of magnetic clusters (cluster glass) below $\simeq 92$ K.

The Fe-Al magnetic phase diagram shows[3,4] that this cluster-glass region extends from Fe_3Al almost to the equiatomic composition. The behavior for the equiatomic composition is generally classified[5] as a Curie-Weiss type paramagnetism, which implies the existence of disordered finite local moments. In addition, some studies[6] conclude that the equiatomic composition is AF and therefore offers the possibility of a temperature-induced transition from AF to FM spin order as is observed[7] in FeRh.

Chemical disorder makes interpretation of the experimental properties of iron-rich Fe-Al alloys somewhat difficult. For example, increasing the chemical disorder by cold-working the equiatomic composition produces FM behavior,[6] possibly caused by the creation of Fe-Fe near neighbors. However, the consensus is that structurally-ordered FeAl exhibits no magnetic order, even at zero temperature. In contrast, FeV is found[8] to be FM with a moment of $\simeq 0.7\mu_B$ per formula unit. We maintain that the experimental ground state of FeAl is still an open question, and will present an argument supporting a magnetic ground state based on the observation that the experimental bulk modulus is much closer to that expected from the FM rather than the NM theoretical bulk modulus.

Conventional spin-polarized band calculations (based on a two-atom magnetic unit cell, which excludes the possibility of AF iron coupling) find[9–11] that ordered FeAl is FM. Since experiment does not find a FM state, it is useful to verify this theoretical result before attempting to explain the experimental result in terms of a cluster-glass model. Our recent success[7,12] in understanding the magnetic structures of FeRh and FeV, both of

which have the same $B2$ structure as FeAl gives us confidence in the reliability of our first-principles methods and motivated the present study of ordered FeAl and FeV. In view of the suggestion[6,13] that FeAl might be AF and that our previous work on FeV only considered two-atom magnetic cells, we extend the calculations to larger magnetic cells to permit AF spin configurations.

Our present work on FeAl and FeV is similar to our work on FeRh, i.e., we use band calculations based on the augmented-spherical-wave method to compute total energies of different magnetic cells as functions of the total magnetic moment of the cell using a fixed-spin-moment procedure. This procedure allows us to find and separate the different solutions to the Kohn-Sham band equations which correspond to NM, FM, and AF spin configurations and to determine the relative stability of these different magnetic states.

II. PROCEDURE

Our total-energy band calculations utilize the atomic sphere approximation, which assumes sphericalized potentials within Wigner-Seitz spheres. This approximation requires the volume V of the unit cell to be divided into constituent Wigner-Seitz atomic spheres with radii r_{Fe} and r_{Al} for FeAl, such that the sum of the sphere volumes is V. Thus, for the CsCl unit cell, $V=(4\pi/3)(r_{\mathrm{Fe}}^3+r_{\mathrm{Al}}^3)=a^3$, where a is the lattice constant. This division can be made in several ways. One can fix the ratio $R=r_{\mathrm{Al}}/r_{\mathrm{Fe}}$ to be unity (equal radii) or can use the ratio of the radii found in the constituent elemental forms. Another method, used by Okochi[14] in augmented-plane-wave calculations on FeAl (non-spin-polarized and only at the experimental lattice constant), matched the potentials at the contact point of the constituent spheres and found $R=1.01$. Ziesche *et al.*[15] used $R=1.06$ (non-spin-polarized and at the experimental lattice constant).

In our calculations we required that the total energy be a minimum with respect to R. Near the equilibrium volume this minimum corresponds to a FM state and to $R=0.95$ for FeAl. All of the FeAl results presented here correspond to this ratio of aluminum to iron sphere radii, although selected calculations using equal radii spheres yielded no significant changes in the calculated results. These results will be presented in terms of an effective radius, r_{eff}, defined by $r_{\mathrm{eff}}^3\equiv(r_{\mathrm{Al}}^3+r_{\mathrm{Fe}}^3)/2$. Our FeV calculations were all done for equal iron and vanadium radii, and will be presented in terms of the common Wigner-Seitz radius, r_{WS}. We note that although elemental aluminum has a larger Wigner-Seitz radius than elemental iron, suggesting that the ratio R for FeAl is larger than unity, we find the surprising result that a ratio less than unity yields lower energies. Our FeAl ratio may be compared with the ratio for Ni_3Al, where we found[16] that the aluminum radius was 8% larger than the nickel radius, but reduced from the 15% larger value of elemental aluminum compared to elemental nickel. The Wigner-Seitz radii appropriate to binary compounds are expected to depend on the details of the bonding and on the values of the elemental bulk moduli of the constituents. Thus, one can expect the aluminum radius to be more easily changed than the iron radius because elemental aluminum has a lower bulk modulus than elemental iron.

III. RESULTS

Four-atom cell calculations yield magnetic structures for FeAl and FeV that are remarkably similar. We find metastable type-I AF solutions a few mRy above stable FM solutions for both systems for volumes near the respective equilibrium volumes. In addition, for FeV we find an unstable AF state with iron and vanadium lattices having equal and opposite moments.

A. FeAl

Ordered FeAl has the CsCl structure with an experimental lattice constant[17] of 5.496 a.u. corresponding to $r_{\mathrm{eff}}=2.707$ a.u. Our calculations span the volume range corresponding to lattice constants within $\simeq\pm5\%$ of equilibrium. Calculations using two-, four-, and eight-atom magnetic cells are used to search for NM, FM, and type-I and type-II AF solutions. The details of the magnetic cells used in the present study are discussed in previous work.[7]

Two-atom magnetic cell calculations constrain binary systems to have either NM or FM spin configurations (the local moments on the constituents can be different, and either parallel or antiparallel). Our calculations yield only stable NM solutions below, and only stable FM solutions above a transition volume corresponding to $r_{\mathrm{tr}}\equiv r_{\mathrm{eff}}\simeq2.546$ a.u. for two-atom cells. For the FM state, a weak local moment ($<0.05\mu_B$) is found on the aluminum sites. The magnetovolume transition from NM to FM behavior at r_{tr} is second order (the magnetic moment is continuous).

Four-atom magnetic cell calculations remove the constraint mentioned above, and allow the more complex type-I (and type-II) AF, in addition to the NM and FM spin configurations. As in our previous work,[7] we constrain the chosen magnetic cell to have fixed values of total magnetic moment M, and compute the total energy and local moments as M is increased or decreased in small steps. From previous experience, we have found that the system can remain in a metastable state if the steps are small enough. We call this procedure adiabatic tracking. Plots of the calculated total energy E and local magnetic moments m_{Fe} vs total moment M for several r_{eff} values are shown in Figs. 1 and 2. The $E(M)$ curves resulting from our fixed-spin-moment constraint procedure describe the behavior of the chosen magnetic cell in an effective applied magnetic field H, defined by $H\equiv dE/dM$. Therefore, solutions at $dE/dM=0$ are special solutions corresponding to states of the system in zero applied magnetic field. Such states can be stable or metastable (positive curvature) or unstable (negative curvature). The NM, FM, and AF zero-field spin configurations, determined by the details of the calculated local moments, are labeled. In all cases, we show two $E(M)$ curves. The solid curves correspond to positive

adiabatic tracking (increasing M) while the dashed curves correspond to negative adiabatic tracking (decreasing M).

As the figures show, the lowest minima in the $E(M)$ curves for volumes V corresponding to $r_{\text{eff}}=2.6733$ and 2.7318 a.u. belong to FM solutions. This is shown by the corresponding local iron moments in the top panels of the figures. The local aluminum moments, which are antiparallel and very weak, are not shown. This FM solution is the minimum-energy solution for all $r_{\text{eff}}>r_{\text{tr}}=2.546$ a.u. The resulting zero-field $E(V)$ curves for these FM solutions and the low-volume NM solutions are shown in Fig. 3, where we see that the equilibrium volume is at $r_{\text{eff}}\simeq 2.658$ a.u. (corresponding to a lattice constant of 5.398 a.u.) and that the theoretical bulk modulus is 1900 kbar. This calculated bulk modulus is larger than the experimental value of 1500 kbar determined[18] from measurements of elastic constants on iron-rich Fe-Al alloys and by extrapolation to the 50%-50% ordered system.

Our theoretical bulk modulus of 1900 kbar, derived from the FM solutions, is $\simeq 27\%$ larger than experiment. This discrepancy can be compared with our value[12] for bcc Fe where the theoretical bulk modulus is 19% larger than experiment. However, the bulk modulus calculated from our (unstable) zero-field NM solutions is 2015 kbar, which is 34% larger than experiment. Thus we find that our theoretical FM bulk modulus agrees better with the value expected from experiment than does our NM bulk modulus. This result suggests that experimentally, FeAl may have finite local moments. Both FM and AF states have similar expanded lattice constants and reduced bulk moduli at equilibrium compared to the NM state.

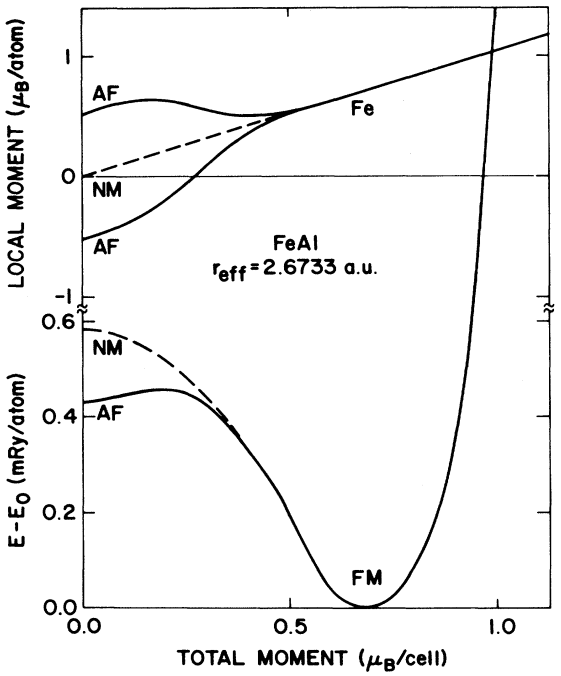

FIG. 1. Total energy (lower panel) and local iron moments (upper panel) vs constrained magnetic moment for FeAl at $r_{\text{eff}}=2.6733$ a.u. showing stable FM, metastable AF, and unstable NM zero-field solutions. E_0 is the minimum energy for this r_{eff} value. The upper panel shows the AF local iron moments. With increasing M value, the two local iron moments merge and assume a FM (parallel spin) configuration. The dashed curves correspond to inverse adiabatic tracking (see text) and reveal the unstable NM zero-field solution at $M=0$.

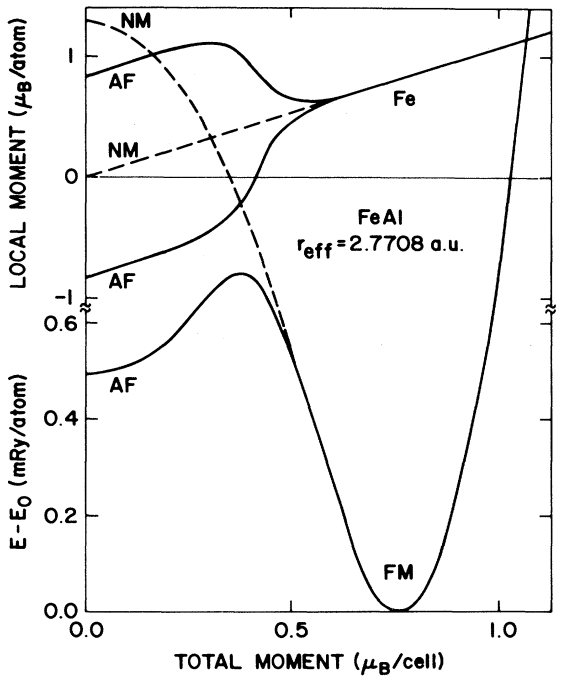

FIG. 2. Total energy (lower panel) and local iron moments (upper panel) vs constrained magnetic moment for FeAl at $r_{\text{eff}}=2.7708$ a.u. showing stable AF and FM zero-field solutions and the unstable NM zero-field solution.

As shown in Figs. 1 and 2, the AF solutions (the solutions at $M=0$) are metastable relative to the lower-energy FM solutions, with differences in total energies of only a few tenths of a mRy. With decreasing volume, the $m_{\text{Fe}}(M)$ curves collapse and finally merge into the dashed NM branch at $r_{\text{eff}}\simeq 2.64$ a.u. Also at $r_{\text{eff}}\simeq 2.64$ a.u., the AF minimum in the $E(M)$ curves merges with a NM maximum. The spin polarization energy per atom, or the energy gained by allowing the system to be FM (two-atom magnetic cells) or to be AF (four-atom magnetic cells), is shown in Fig. 4. As indicated, the FM total energy at equilibrium (r_0) is almost 0.5 mRy lower than the NM total energy. At the same volume, the AF total energy is $\simeq 0.1$ mRy lower than the NM total energy.

The FM and AF local moments are shown in Fig. 5, where we again see that the magnetovolume transition from NM to FM behavior occurs at $r_{\text{tr}}\simeq 2.546$ a.u., and that AF solutions occur for $r_{\text{eff}}>2.64$ a.u. Note that in the case of the NM to FM transition at 2.546 a.u., the transition is from a stable NM state to a stable FM state. In the case of the NM to AF transition at 2.64 a.u., the transition is from an unstable NM state to a metastable AF state, hence this is not an observable transition.

We note that the calculations yield small residual AF local moments for $r_{\text{eff}}<2.64$ a.u. leading to a tailing-off of

the AF m_{Fe} curve in Fig. 5. Past experiences with simpler systems suggest that this tailing-off is not physically correct and results from computational errors caused by the lack of k-space convergence, and that the correct behavior should exhibit the singular behavior[19] shown by the dashed curve.

Repeated attempts to find type-II AF solutions in the volume range covered in Fig. 3 were unsuccessful. Constraining the system to type-II AF by forcing nearest-neighbor iron atoms in (100) planes to be antiparallel initially, always resulted in zero local iron moments for the $M=0$ case, and equal and parallel local moments for $M\neq 0$.

B. FeV

As we have already shown,[12] FeV at equilibrium ($r_{WS}=2.661$ a.u.) is FM, but with a local iron moment much reduced from that of elemental bcc Fe. The local vanadium moment is small and parallel to the iron at low volumes, is nearly zero at equilibrium, and becomes large and antiparallel to the iron at large volumes. At equilibrium, the local iron moment is $0.66\mu_B$. Our calculated lattice constant is within 1.4% of the experimental value. The present work uses larger magnetic cells and thereby focuses on the possibility of various kinds of AF solutions, which were excluded in our previous work.

In Fig. 6 we show the total energy and local iron and vanadium moments vs the constrained total moment for FeV at a volume corresponding to $r_{WS}=2.70$ a.u. (with equal iron and vanadium radii). This r_{WS} corresponds to a lattice constant $\simeq 1.5\%$ greater than the calculated

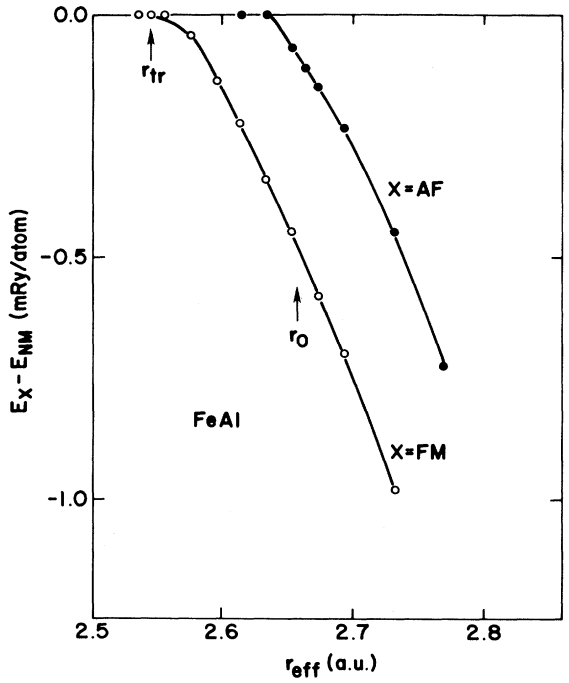

FIG. 4. Spin-polarization energies for the FM (two-atom magnetic cell, open points) and AF (four-atom magnetic cell, solid points) zero-field solutions for FeAl. The magnetovolume transition from NM to FM behavior occurs at $r_{tr}=2.546$ a.u. The zero-pressure solution at $r_0=2.658$ is FM.

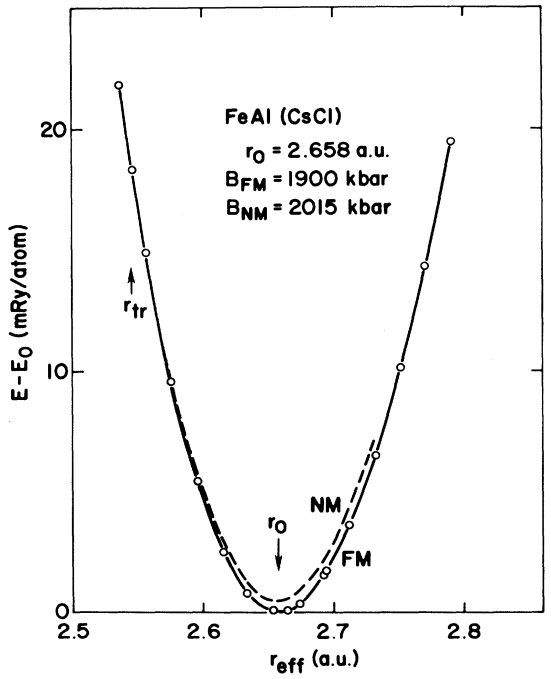

FIG. 3. Zero-field total energy vs r_{eff} for the minimum energy FM solutions (points) and NM solutions (dashed line) for FeAl. Metastable AF solutions are not shown here. Analysis of the $E(r_{eff})$ FM curve yields the zero-pressure equilibrium point at $r_0=2.658$ a.u., and a bulk modulus of 1900 kbar. Analysis of the $E(r_{eff})$ NM curve yields approximately the same zero-pressure equilibrium point, and a bulk modulus of 2015 kbar. The magnetovolume transition from NM to FM behavior occurs at $r_{tr}=2.546$ a.u.

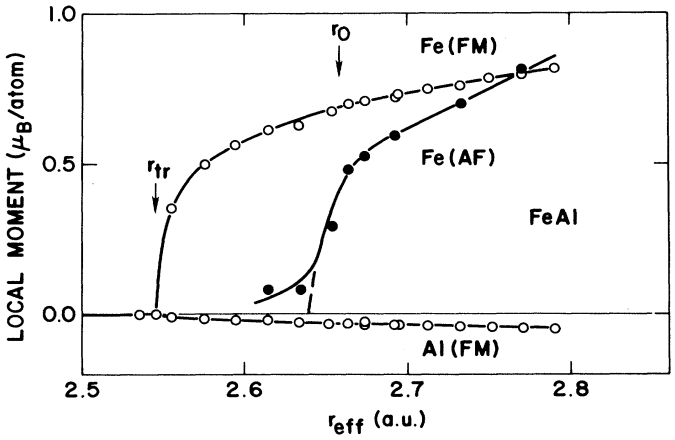

FIG. 5. Local moments for the FM (open points) and the AF (solid points) zero-field solutions for FeAl. The zero-pressure volume corresponds to r_0. The AF solutions yield no local moments on the aluminum sites. The magnetovolume transition from NM to FM behavior occurs at $r_{tr}=2.546$ a.u.

equilibrium lattice constant. This result was obtained by assuming that the two iron atoms had independently variable moments, but that the two vanadium atoms always had identical moments. Calculations which removed the constraint on the vanadium atoms and allowed them to be different failed to converge to self-consistency.

As shown in Fig. 6, we find a stable FM state for the $M \simeq 0.68\mu_B$/unit cell with most of the moment on the iron sites. For this state and at this volume, we find a small $\simeq 0.15\mu_B$ local moment on the vanadium atoms. At $M=0$, we find a well-defined local minimum where the local iron moments at $\pm 0.72\mu_B$, corresponding to a metastable AF state, which we call AF_1. In this case, the vanadium local moment is $\simeq$ zero. Positive adiabatic tracking leads to a merging of the two local iron moments at $\simeq 0.6\mu_B$/unit cell accompanied by a slight negative local moment on the vanadium. Above $0.6\mu_B$, the vanadium local moment increases, following the local iron moments. For negative adiabatic tracking, we return to another (unstable) AF mixed state at $M=0$, which corresponds to local iron moments of $+0.42\mu_B$ and local vanadium moments of $-0.42\mu_B$. That is, we find an unusual *unstable* AF state consisting of equal but antiparallel iron and vanadium moments, which we call

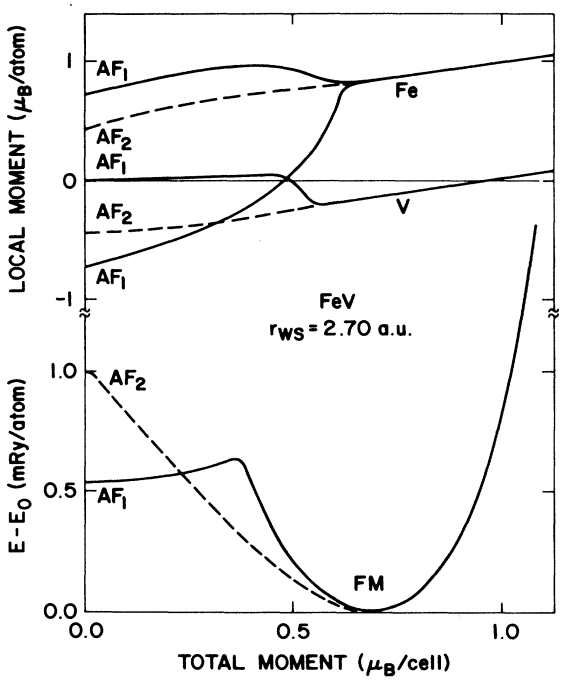

FIG. 6. Total energy (lower panel) and local iron and vanadium moments (upper panel) vs constrained magnetic moment for FeV at $r_{WS}=2.70$ a.u. showing stable FM, metastable AF_1, and unstable AF_2 zero-field solutions. E_0 is the minimum energy for this r_{WS} value. The upper panel shows the AF_1 local iron moments for low M values. With increasing M value, the two local iron moments merge and assume a FM (parallel spin) configuration. The dashed curves correspond to inverse adiabatic tracking (see text) and reveal an unstable AF_2 zero-field solution at $M=0$.

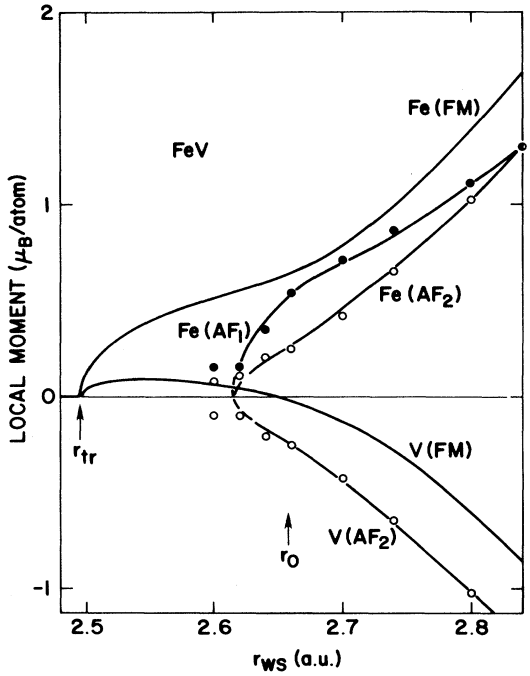

FIG. 7. Local moments corresponding to zero-field solutions for FeV. The solid lines are for the FM solutions from Ref. 12. The solid points are the local iron moments for AF_1 solutions with vanishingly small local vanadium moments, and the open points are the iron and vanadium moments for AF_2 solutions with equal and opposite iron and vanadium moments. The zero-pressure volume corresponds to $r_0=2.658$ a.u. The magnetovolume transition from NM to FM behavior occurs at $r_{tr}=2.494$ a.u.

AF_2. This unstable AF_2 state is analogous to the unstable AF state found for elemental bcc iron.[20]

The volume dependence of the local iron and vanadium moments for the FM, AF_1, and AF_2 states for FeV are shown in Fig. 7. The FM local moments are from Ref. 12. The AF_1 and AF_2 solutions both begin at $\simeq 2.62$ a.u., just below the zero pressure volume at $r_0=2.658$ a.u. The details of the termination of the AF solutions at 2.62 a.u. is not clear. In this region the FM solutions are more stable.

The relative stability of the three types of solutions for FeV is implied in Fig. 8 where we show the spin-polarization energy, or the energy difference between the nonmagnetic solutions and the various magnetic solutions. The FM results are similar to our earlier results[12] for all but the largest volumes, but are plotted as negative quantities. In general, the FM solutions are more favored (have a lower energy) than the AF_1 solutions, which are more favored than the AF_2 solutions (which are unstable). Thus the FM solution is favored at r_0. The large-volume behavior of the AF_2 solutions is uncertain. We note that, although Fig. 7 shows both AF_1 and AF_2 solutions terminating near 2.62 a.u., Fig. 8 shows that the energy difference between the NM and the AF_2 solutions in

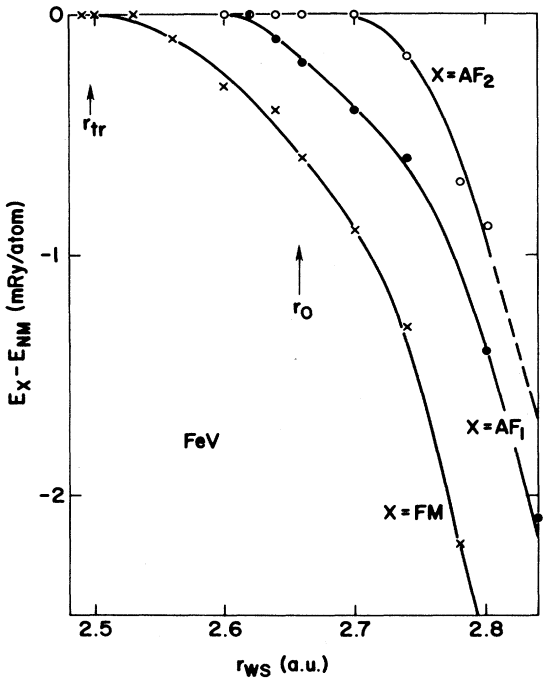

FIG. 8. Spin-polarization energies for the FM (two-atom magnetic cell, x points), the AF_1 (four-atom magnetic cell, solid points), and the AF_2 (four-atom magnetic cell, open points) zero-field solutions for FeV. The magnetovolume transition from NM to FM behavior occurs at $r_{tr}=2.494$ a.u. The zero-pressure solution at $r_0=2.658$ is FM.

the region from 2.62 to 2.70 a.u. is less than the resolution of the present calculations.

IV. DISCUSSION

The ordered FeAl and FeV results presented above are similar to results obtained for ordered FeRh. In both cases, we find FM and AF stable or metastable states. Near equilibrium, we find the AF state more stable than the FM state for FeRh, but the FM state more stable than the AF state for FeAl and FeV. The energy differences between the two states are a few mRy for FeRh, but only a few tenths of a mRy for FeAl and FeV. But we have shown that zero-point energy corrections are important for FeRh, and reduce the energy difference between the two competing states to 0.3 mRy. Hence the formation of magnetic clusters in these systems seems plausible.

In Table I we compare the equilibrium properties of four B2 systems for which first-principles total-energy calculations have been made, i.e., FeAl, FeV, FeFe (bcc Fe), and FeRh. The entries are in order of increasing magnetic activity. Both FeAl and FeV have small FM and AF moments, but FeV also has a mixed AF_2 state in which the vanadium acquires a moment antiparallel to the iron moments. Apparently, the ability of vanadium to acquire a moment (in contrast to aluminum) allows a greater variety of magnetic structures. Note that $E_{AF}-E_{FM}$ is greater for the AF_2 state than for the AF_1 state, which has vanishingly small local vanadium moments. This mixed AF_2 state therefore has a higher (less favorable) energy. Although this AF_2 state is unstable and reverts to the FM state when the $M=0$ constraint is relaxed, it indicates a new magnetic tendency that could become metastable. This same tendency is found in bcc Fe, with larger moments. In FeRh, the AF tendency is further enhanced, since the ground state is now AF, but takes a different direction by becoming type II, in which iron atoms have an AF arrangement within, as well as between, (100) planes. Comparing the binary compounds with FeFe, we see that both aluminum and vanadium tend to reduce the local iron moments, while rhodium tends to enhance them. This behavior is readily understood in terms of reducing the number of majority-spin electrons in the former case but increasing it in the latter case.

In summary, we find FM ground states for both ordered FeAl and FeV. Our result is in contradiction with the experimental finding that FeAl is NM, but we note that the energy differences are very small and that our FM bulk modulus is in better agreement with experiment

TABLE I. Theoretical equilibrium properties for some iron binary compounds in the B2 structure. Local moments are designated as m_S^X, where S signifies the state (FM or AF) and X signifies the constituent (Al, V, Fe, or Rh). $E_{AF}-E_{FM}$ is the rigid-lattice energy difference between the AF and FM state (with no zero-point correction).

System (FeX)	r_0 (a.u.)	Ground state	B (kbar)	m_{FM}^{Fe} (μ_B)	m_{AF}^{Fe} (μ_B)	m_{FM}^{X} (μ_B)	m_{AF}^{X} (μ_B)	$E_{AF}-E_{FM}$ (mRy/atom)
FeAl	2.658	FM	1900	0.7	0.4	0.0	0.0	0.5
FeV	2.661	FM	2320[a]	0.7	0.7	0.0	0.0	0.5
FeV[b]					0.4		0.4	0.7
FeFe[a]	2.631	FM	2053[a]	2.1	1.7[c]	2.1	1.7[c]	30
FeRh[d]	2.782	AF	2144	3.1	2.9	1.0	0.0	−2

[a]Reference 12.
[b]AF_2 solutions (see text).
[c]Reference 20. Estimated from unstable AF state at $r_{WS}=2.70$ a.u.
[d]Reference 7.

than our NM bulk modulus. For both FeAl and FeV, we find close-lying AF states a few tenths of a mRy above the FM ground states. In addition, we show the existence of a new type of AF state in FeV, which is unstable but which can influence fluctuation and excitation behavior.

ACKNOWLEDGMENT

We are indebted to D. Singh for bringing the FeAl problem to our attention and for many helpful discussions.

[1]J. W. Cable, L. David, and R. Parra, Phys. Rev. B **16**, 1132 (1977).
[2]R. D. Shull, H. Okamoto, and P. A. Beck, Solid State Commun. **20**, 863 (1976).
[3]K. Motoya, S. M. Shapiro, and Y. Muraoka, Phys. Rev. B **28**, 6183 (1983).
[4]H. Wada, Y. Muraoka, M. Shiga, and Y. Nakamura, J. Phys. Soc. Jpn. **54**, 2700 (1985).
[5]K. Miyatani and S. Iida, J. Phys. Soc. Jpn. **25**, 1008 (1968).
[6]A. Arrott and H. Sato, Phys. Rev. **114**, 1420 (1959).
[7]V. L. Moruzzi and P. M. Marcus, Phys. Rev. B **46**, 2864 (1992).
[8]R. J. Chandross and D. P. Shoemaker, J. Phys. Soc. Jpn. **17**, Suppl. B-III, 16 (1962).
[9]B. I. Min, T. Oguchi, H. J. F. Jansen, and A. J. Freeman, J. Magn. Magn. Mater. **54-57**, 1091 (1986).
[10]O. Eriksson and A. Svane, J. Phys. Condens. Matter **1**, 1589 (1989).
[11]O. Eriksson, L. Nordström, A. Pohl, L. Severin, A. M. Boring, and B. Johansson, Phys. Rev. B **41**, 11 807 (1990).
[12]V. L. Moruzzi and P. M. Marcus, Phys. Rev. B **45**, 2934 (1992).
[13]H. Sato and A. Arrott, Phys. Rev. **114**, 1427 (1959).
[14]M. Okochi, J. Phys. Soc. Jpn. **39**, 367 (1975).
[15]P. Ziesche, H. Wonn, Ch. Müller, V. V. Nemoshkalenko, and V. P. Krivitskii, Phys. Status Solidi B **87**, 129 (1978).
[16]V. L. Moruzzi and P. M. Marcus, Phys. Rev. B **42**, 5539 (1990).
[17]From *Crystallographic Data on Metal and Alloy Structures,* compiled by A. Taylor and B. J. Kagle (Dover, New York, 1963).
[18]H. J. Leamy, Acta Metall. **15**, 1839 (1967).
[19]V. L. Moruzzi, Phys. Rev. Lett. **57**, 2211 (1986).
[20]V. L. Moruzzi and P. M. Marcus, Phys. Rev. B **42**, 8361 (1990).